Preferred citation: F. Le Gallic, M. Teil, J. Viguié, C. Martin and R. Passas. Wrinkles formation and origins: from theory of web handling to coating pilot scale experimentation. In *Advances in Pulp and Paper Research*, Cambridge 2022, Trans. of the XVIIth Fund. Res. Symp. Cambridge, 2022 (D. Coffin and W. Batchelor, eds), pp 391–420. FRC, Manchester, 2022. DOI: 10.15376/frc.2022.1.391.

WRINKLES FORMATION AND ORIGINS: FROM THEORY OF WEB HANDLING TO COATING PILOT SCALE EXPERIMENTATION

Florian Le Gallic, Maxime Teil, Jérémie Viguié, Céline Martin and Raphaël Passas*

Univ. Grenoble Alpes, CNRS, Grenoble INP (Institute of Engineering Univ. Grenoble Alpes), LGP2 (Laboratoire de Génie des Procédés Papetiers) F-38000 Grenoble, France

ABSTRACT

When coating lightweight grade paper with aqueous coating color, wrinkles could appear on roll to roll coating system. This study is conducted from fundamental and theoretical point of view to laboratory experiments. The impact of water content will be taken in count. It has been experimentally observed that the appearance of wrinkles during a coating process on a roll to roll pilot depends on different parameters: web tension; misalignment angle; the coefficient of friction between the roll and the side of the paper in contact; the water content in the paper that appears to favour the wrinkles formation. Moreover, this work highlights the impact of discretisation of the variable represented wrinkles number i on the prediction model. Initial tests of the use of DIC during a tensile test have been carried out. These initial tests are very promising and the development of this technique is currently being developed. The perspective of this work is the improvement of the DIC study on the formation of out-of-plane displacement during the coating process. It can reduce the cost of non-conformities and thus reduce the waste of raw materials.

* Corresponding author

1 INTRODUCTION

Since its creation, paper as a material has constantly evolved to meet society's needs. Currently, research on paper focuses in the reduction of grammage with constant mechanical characteristics and the functionalization of papers. The goals of these researchs are to decrease the environmental footprint of the paper mills, and to obtain specific surface properties (barrier properties . . .). These characteristics can be obtained by coating. This process use roll to roll technology that is widely found in many industries due to its high efficiency and low production cost. However, before being converted to the final product, paper web goes through several conversion operations. The quality of the deposited layer depends on the triplet: paper/layer formulation/process [1]. The main controlled parameters are: the quantity of coating color deposed, the travel time from coating to drying and the drying conditions. Furthermore, when coating very lightweight papers, wrinkles may appear at the exit of the coating area. After drying and depending on the coating color, they could be irreversible and cause runnability issues [2] and downgrading of the products (Figure 1). Thus, the web tension and the rollers alignment must be mastered to keep a perfectly flat web.

Wrinkling is a common and costly web defect encountered in the manufacturing and converting of lightweight grades of paper, film and textiles. A lot of synonyms exist: baggy lane, creases, troughs, soft/hard wrinkles . . . According to Walker [3] the following terms will be used as follows: a web trough is an out-of-plane deformation of the web that occurs between rollers in web-handling system. A web wrinkle is an out-of-plane deformation of the web that is transferred over rollers from one web span to the next. Wrinkling appears in several stages. Firstly, the water, coming from the coating color, goes into the fiber network, causing a reduction in mechanical properties especially the Young's modulus. This water absorption increases the instability issues already present (low thickness and low bending stiffness of the web). Secondly, the loading imposed by the web tension may be non-uniform across the web and leads to troughs or wrinkles. Web troughs

Figure 1. Conformed (left) and non-conformed paper (right).

can be caused by various factors including roller misalignment, imperfect roller profile, non-uniform tension, uneven web cross-section and friction force between paper and roller [4]. Roller misalignment has one of the most significant impact on troughs or wrinkles formation. It leads to non-uniform distribution of the load that generates secondary compressive stresses perpendicular to the paper transport direction and creates an out-of-plane deformation in the free span. When it passes from a web span to another it becomes a wrinkle (on the roller). Furthermore, when this buckled paper passes over the roll it will create permanent creases. Troughs can be avoided by increasing the applied global tension or by reducing the roller misalignment. However, over high precision of roller parallelism can greatly increase the cost of roll to roll system and an overlarge tension could break the web [5]. Last but not least, the complexity of the entire mechanical/moisture/temperature history of the web submitted to coating raise a challenge.

In this study, fundamental and theoretical work on web wrinkling is conducted and applied on the case of wrinkles appearances during an aqueous coating process. The impact of water content will also be investigated to understand its role in wrinkles formation. The discretization of the variable representing the number of wrinkles will be discussed to know its impact on the wrinkle occurrence model. In addition, the possibility of using a buckling coefficient to help design a roll-to-roll installation will be analysed. The use of Digital Image Correlation (DIC) will be considered to monitor the formation of wrinkles during tensile tests or during the coating process for production control.

2 THEORETICAL CONSIDERATIONS

2.1 A Brief Sum-up of Wrinkles Study

The study of wrinkles on a moving web is not new. The theory setting out the foundations for studying this problem was proposed by Leonhard Euler, around 1750, who formulated a first theory of beams by defining the *elastica*, a medium or neutral fiber that deforms in flexion without contracting or compressing. The study of plate bending returned during the 19th century with the studies of Young, Laplace, Poisson, Navier, Cauchy, Fourrier, Germain, Lamé and Clapeyron. In 1888, Love used the assumptions of Gustav Kirchhoff, themselves inspired by the Euler-Bernoulli assumptions for beams, to found a theory of thin plates. The plate theory was consolidated by Rayleigh (1877), von Kármán (1910), Timoshenko (1921), Reissner (1945) and Uflyand (1948). It's important to note that in the literature, the Timoshenko's theory of elastic stability is frequently found and cited as well as Föppl–von Kármán equations that described large deflections of thin flat plates. The physical validity of these last equations stay questionable [6].

It is then possible to draw a parallel between a plate and a web. It is known in the web handling industries that web wrinkles come from misaligned rollers. Therefore, many investigators formulated the prediction model of wrinkles for isotropic webs with constant Young's modulus in machine direction (MD) and cross direction (CD). Generally, the instability problem of tensioned webs can be solved by two approaches. The first one is the tension field theory. It offers a convenient criterion of the critical load and uses the beam theory. However, this theory ignores the bending stiffness of webs, thus the calculated critical buckling load is always underestimated.

The second method is the plates buckling theory, which considers the webs as plates with low bending stiffness. Analyses have been done using the energy methods or numerical methods such as finite element analysis [7]–[11]. Shelton [12] studied the boundary conditions of webs transported through misaligned rollers: webs were modelled as Euler beams, and the normal entrance law was proposed to determine the boundary conditions. Then, the stress distribution in the web could be obtained. Furthermore, based on Shelton's studies, many other buckling analyses of webs have been done and published. For example, a series of studies were carried out in the Web Handling Research Center (Oklahoma State University, USA). In 1989, experimental investigations show that two types of wrinkling failures can exist in webs subjected to shear due to roller misalignment [13]. Good et al. [14] presented a buckle prediction model for isotropic webs with roller misalignment, which reliably forecasted the web behaviour. However, anisotropic materials such as paper, have different Young's modulus in MD and CD. Moreover, in the case of paper-webs, the web air permeability could impact wrinkles formation. Accordingly, Good and Beisel analysed the mechanism of buckling of anisotropic PET rolls. Hashimoto [15] proposed a theoretical modelling of paper-web wrinkling generation due to misalignment of roller and also considered web speed and web tension. It is completed with experimental verifications. Beisel [16] studied the buckling phenomenon caused by the imperfect structure of rollers, such as coin or concave profile of rollers. Moreover, Good and Beisel [4] used the biaxial loaded plates buckling criterion to study the buckling of the web caused by the misalignment of the roller. These theories have been used by Martz in his PhD thesis [10] where he also proposed a table that sums up the impact of each process parameters. Cerda et al. [17] studied the instability problem of webs/plates with two opposite edges clamped and subjected to uniform tension. Same work have been done by Zhu et al. [18]. However, in all these previous studies webs were modelled as plates subjected to uniform biaxial loads, which did not conform to the practical stress distributions in the webs. Thus, Kim Lin and Mote [19]–[21] studied the critical buckling loads of webs with all edges simply supported and subjected to non-uniform tension. Tang et al. [5] proposed a theoretical calculating process for the elastic buckling of webs transported through a

pair of misaligned rollers, by making use of the plate buckling theory and determining the stress distribution of webs by using the Timoshenko beam theory.

2.2 Theoretical Models

Webs are composite membranes and plate structures that react to compressive stresses until they reach the critical buckling stress [22], [23]. Wrinkles in web are caused by the compression exceeding the critical buckling stress (when plates don't shorten but bend) and can be loaded in three directions. In this case, the focus is made on wrinkles, with machine direction web tension, induced by lateral shearing forces in the web, and the wrinkles that result are called "shear wrinkles" (Figure 2). Timoshenko proposed a solution for the buckling stresses for a rectangular plate [24]. It allows tension on two opposing sides and compression on the other two opposing sides.

Assuming that the plate buckles slightly under the forces applied in its middle plane and then to calculate the magnitudes that the forces must have in order to keep the plate in such a slightly buckled shape. The energy method is used to solve this problem of plates buckling. Noting ΔT the work of external forces acting on the plates and by ΔU the strain energy of bending, the critical values of forces could be found as:

$$\Delta T = \Delta U \tag{1}$$

➢ *Isotropic materials (Timoshenko's theory):*

Introducing forces N_x, N_z, the Poisson's ratio for an isotropic material ν_{iso}, the web bending stiffness D_{iso} and out of plane displacements w, it leads to:

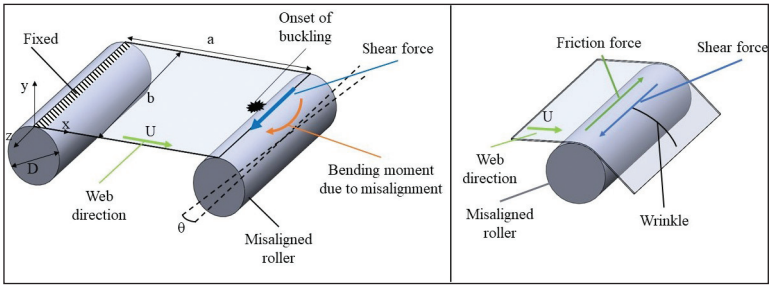

Figure 2. Buckling generation by shearing (left) and impact of friction force (right) [15].

$$\int -\frac{1}{2}\left[N_x\left(\frac{\partial w}{\partial x}\right)^2 + N_z\left(\frac{\partial w}{\partial z}\right)^2\right]dx\,dz = \frac{D_{iso}}{2}\left\{\left(\frac{\partial^2 w}{\partial x^2}+\frac{\partial^2 w}{\partial z^2}\right)^2 \int -2(1-\nu_{iso})\left[\frac{\partial^2 w}{\partial x^2}\frac{\partial^2 w}{\partial z^2}-\left(\frac{\partial^2 w}{\partial x \partial z}\right)^2\right]\right\}dxdz \tag{2}$$

Assuming that x-direction is MD and z-direction is CD, $w_{mn}(x,y) = w$ could be described as the solution of linear partially differential equation and a_{mn} is the amplitude [24].

$$w_{mn}(x,y) = a_{mn} sin\left(\frac{m\pi x}{a}\right) sin\left(\frac{n\pi z}{b}\right) \tag{3}$$

It is assumed that the edges of the plates are simply supported. *b* is the web width (mm), *a* the web span (mm). The number of half waves in the x-direction is *m*, and in z-direction in *n*. Thus, combining the previous equation, dividing by the web thickness t_f and introducing the stress yield σ_x and σ_z:

$$N_x\left(\frac{m\pi}{a}\right)^2 + N_z\left(\frac{n\pi}{b}\right)^2 = D_{iso}\left[\left(\frac{m\pi}{a}\right)^2 + \left(\frac{n\pi}{b}\right)^2\right]^2 \tag{4}$$

$$\sigma_x m^2 + \sigma_z\left(n\cdot\frac{a}{b}\right)^2 = \sigma_{e,iso}\left[m^2 + \left(n\cdot\frac{a}{b}\right)^2\right]^2 \tag{5}$$

where:

$$\sigma_{e,iso} = \frac{\pi^2 D_{iso}}{a^2 t_f} \tag{6}$$

Setting *m = 1* because only one-half wave appeared in MD direction, the previous equation become:

$$\sigma_x + \sigma_z\left(n\cdot\frac{a}{b}\right)^2 = \sigma_{e,iso}\left[1+\left(n\cdot\frac{a}{b}\right)^2\right]^2 \tag{7}$$

This last equation is the basic equation for failure criteria used to indicate if wrinkling appeared on the web. Finally, after some calculation, for an isotropic plate, it leads to the critical normal stress necessary to generate wrinkles $\sigma_{z,cr}$, where *i* is the number of half waves for a specific span that is wrinkled:

$$\sigma_{z,cr} = \frac{b^2}{i^2 a^2}\left[\sigma_{e,iso}\left(1+\frac{i^2 a^2}{b^2}\right)^2 - \sigma_x\right] \tag{8}$$

➢ *Orthotropic materials:*

In a similar way, by taking into account the anisotropy of paper, with a thickness t_f (mm), $\sigma_{z,cr}$ is given by [15] according to equation (9):

$$\sigma_{z,cr} = \frac{b^2}{i^2 a^2}\left[\sigma_{e,ortho}\left(1+\xi_1 i^4 \frac{a^4}{b^4}+\xi_2 i^2 \frac{a^2}{b^2}\right) - \sigma_x\right] \tag{9}$$

where:

$$\sigma_{e,ortho} = \frac{\pi^2 D_{xx}}{a^2 t_f} \text{ is the normalized stress for orthotropic plates} \tag{10}$$

$$D_{xx} = \frac{E_x t_f^3}{12(1-\nu_{xz}\nu_{zx})} \text{ is the web bending stiffness in x-direction} \tag{11}$$

$$\xi_1 = \frac{E_z}{E_x}; \xi_2 = \frac{4\left(1-\nu_{xz}\nu_{zx}\right)}{1+\nu_{xz}+\frac{1+\nu_{xz}}{\xi_1}} + \nu_{zx} + \nu_{xz}\xi_1 \tag{12}$$

$$\sigma_x = \frac{T_x}{t_f} \text{ with } T_x \text{ the web tension} \tag{13}$$

E_x and E_z are the elastic modulus (MPa) in x-direction (loading direction and web transport direction) and z-direction (transverse direction), ν_{xz} is the Poisson's ratio for transverse strain in the z-direction ε_z when stretched in the x-direction, where ε_x is the strain in x-direction. Since the ratio E_z/E_x is defined as ξ_1, the Poisson's ratios in the same plane are related due to the symmetry of the stiffness matrix.

$$\nu_{xz} = \frac{-\varepsilon_z}{\varepsilon_x} \text{ and } \nu_{zx} = \xi_1 \nu_{xz} \tag{14}$$

It is possible to determine the maximum critical shear stress that the web must withstand τ_{cr} and link it with the tram error θ (°) (also called misalignment angle) according to equation (3), invoking Castigliano's second theorem:

$$\tau_{cr} = \sqrt{\sigma_{z,cr}^2 - \sigma_x \sigma_{z,cr,}}\ \theta = \frac{6\tau_{cr} a^2}{E_x b^2} \tag{15}$$

Another point to consider is the friction between the paper and the surface of the roll. Indeed, this friction will determine the web tension T at which wrinkles may or may not appear. This critical tension value T_{cr} is inversely proportional to the value of the friction coefficient μ as described in equation (16). Thus, as presented by Hashimoto [15], a simple empirical model is used:

$$T > T_{cr} = \frac{2t_f^2}{\mu b}\sqrt{\frac{E_x E_z}{3(1-\nu_{xz}\nu_{zx})}} \tag{16}$$

Finally, a last point of the theory will be discussed: the buckling coefficient k_c used in literature dealing with plates stability under compressive or shear loading. Knowing the ratio b/a, it is possible to calculate k_c and then to determine the critical compression value $\sigma_{x,\mathrm{cr}}$ for which a plate buckles. In the case of buckling due to constrained edges, a similar formulation can be obtained for critical tensile loading.

$$T_{cr} = k_c \frac{\pi^2 D_{xx}}{b^2} or\, \sigma_{x,cr} = k_c \frac{E_x \pi^2}{12\left(1-\xi_1 \nu_{xz}^2\right)} \cdot \left(\frac{t_f}{b}\right)^2 \tag{17}$$

Thus, the critical tensile stress can be calculated. However, where some papers deal with isotropic films [17], [25]–[27], it is necessary to use a formulation that considers the anisotropy (or orthotropy) of the paper. Thus, based on Zhu et al. [18] work on highly orthotropic films, the following relationship can be used:

$$\sigma_{x,cr} = \frac{E_x \pi^2}{12\left(1-\xi_1 \nu_{xz}^2\right)} \cdot \left(\frac{t_f}{b}\right)^2 \cdot \left\{ \frac{3\xi_1 - 1 + 2\xi_1^2 \nu_{xz}}{\xi_1 + 1 + 2\xi_1 \nu_{xz}} \beta^2 + \xi_1 [\beta^{-2} n^2 (n+2)^2 + n^2 + (n+2)^2] \right\} \tag{18}$$

where $\beta = b/a$.

Thus, k_c can be isolated:

$$k_c \left\{ \frac{3\xi_1 - 1 + 2\xi_1^2 \nu_{xz}}{\xi_1 + 1 + 2\xi_1 \nu_{xz}} \beta^2 + \xi_1 [\beta^{-2} n^2 (n+2)^2 + n^2 + (n+2)^2] \right\} \tag{19}$$

However, this relationship is only valid when the plate is clamped at its ends, contrary to the assumption made by Good where the plate, i.e. the paper, is simply supported and thus generates a different behaviour with respect to the Poisson's effect. Moreover, Juner's work is also based on the Föppl-von Karman equation and must therefore be used with the assumptions of its complexity in mind [6].

Thus, in this study the relationship between the misalignment angle and the web tension (equation 15), as well as the critical web tension (equation 16) will be mostly used. The buckling coefficient (equation 19) will also be studied. Therefore, the mechanical properties of the studied papers must be measured.

3 MATERIALS AND METHODS

3.1 Studied Papers

The paper supplied by the manufacturer is a single-sided coated paper with calcium carbonate and kaolin, with different grammages: 35 and 40 g.m^{-2}. These pigments are bonded with an SBR (Styrene Butadiene Rubber) latex. The two sides of the papers supplied are clearly identifiable on Figure 3.

In addition, to carry out the DIC tests, a random speckle is printed on the industrially coated side. These speckles are needed to make difference between each studied point on the samples. The printing is carried out with a Xerox laser printer at a resolution of 600 DPI. Printed papers are also characterised and compared with non-printed papers.

3.2 Characterisation Methods

In order to determine the characteristics of the papers used, the following methods were used. The grammage (W) of the samples was determined in accordance with ISO 536. The thickness (t_f) of the samples was measured according to ISO 534. In order to determine the Young's modulus in of the papers, the tests were carried

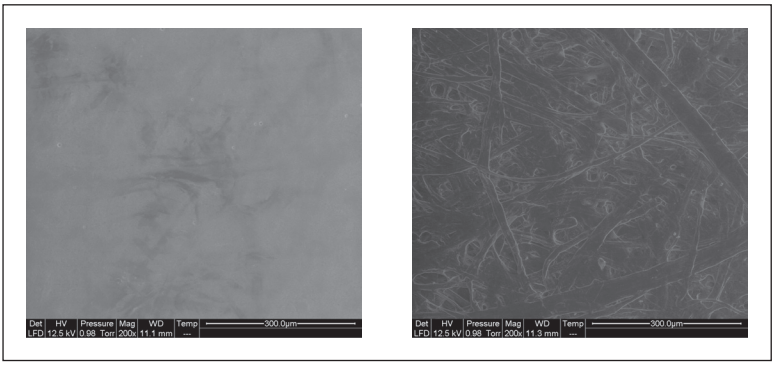

Figure 3. SEM (secondary electrons, low vaccum mode) pictures of the studied paper: coated face (left) and uncoated face (right).

out at a constant tensile speed of 10 mm.min^{-1} in accordance with ISO 1924. Tensile measurements were carried out on an Instron 5965 testing machine with samples of 15 mm width and 100 mm length. All the tests have been done at 23.5 ± 1 °C and 45 ± 5 % HR.

To determine the bending stiffness of the sample, a resonance method is used following the ISO 5629 standard (cf. Figure 4).

The bending stiffness S (mN.m) is obtained as follow:

$$S = 20 \times \left(\frac{l_{res}}{100} \right)^4 \times \frac{W}{100} \tag{19}$$

Where l_{res} is the resonance length (mm). However, this method leads to a high dispersion coefficient for the l_{res} values.

To calculate the Poisson's ratio, 2 methods were used: an empirical model equation and one from mechanics for orthotropic materials. The empirical model equation is used by Biancolini [29] and was first proposed by Baum [30], [31]. This empirical correlation bounds shear modulus and Poisson ratio:

$$G_{xz,Baum} = 0.387\sqrt{E_x E_z} \; and \; \nu_{xz,Baum} = 0.293\sqrt{\frac{E_z}{E_x}} \tag{20}$$

$G_{xz,Baum}$ is the shear modulus in the xz plane determined following Baum's equations. The other method comes from the constitutive equations of mechanics for an orthotropic material and is notably proposed by Viguié [32].Thus, the experimentally measured E_{tan} can be expressed as follows:

$$\frac{1}{E_{tan}} = \frac{1}{E_x} cos^4(\phi) + \left(2\frac{-\nu_{xz}}{E_x} + \frac{1}{G_{xz}} \right) sin^2(\phi) cos^2(\phi) + \frac{1}{E_z} sin^4(\phi) \tag{21}$$

In order to obtain the G_{xz} and ν_{xz} values, it is necessary to measure the tangent modulus of paper samples E_{tan} at a same strain. The fibres in the sample are not

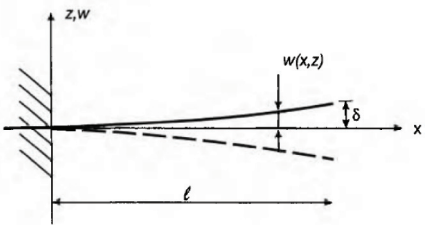

Figure 4. The resonance method. Resonance corresponds to maximum deflection δ [28].

aligned with the measurement direction: ϕ is the angle between the tested direction and MD. Once all the moduli are measured, a fitting between the experimental values and the values was performed by the least squares method.

3.3 Digital Image Correlation (DIC)

The wrinkle formation mechanism was reproduced on an Instron 5965 tensile testing machine to recover displacement and deformation information thanks to 2D and 3D image correlation. Sony Alpha 6000 with a 35–70 (f 3.5–4.5) lens was used for 2D image correlation and two Canon EOS 1200D DSLR (Digital Single-Lens Reflex) cameras with Canon EFS 24mm 2.8 STM lenses for 3D stereo-correlation (cf. Figure 5).

The software used for the tensile is 7D (developped by Pierre Vacher, from Université Savoie Mont-Blanc, France). For the DIC study, the speckled samples were used. The sample were tested in CD and MD for the two different grammages. In the 7D software, an area of interest is defined per set of photos. The algorithm for correlating images is a combination of Harris and Pyramid algorithms.

3.4 Coating Pilot

In order to proceed with the formation of the wrinkles and to study their formation, a Rotary Coater pilot from RK Coating is used (cf. Figure 6). To create troughs and wrinkles, the downstream roll is deliberately misaligned with a known angle (cf. Figure 7). For each angle of misalignment, different web tensions are adjusted using a clamping brake system mounted on the feed roll.

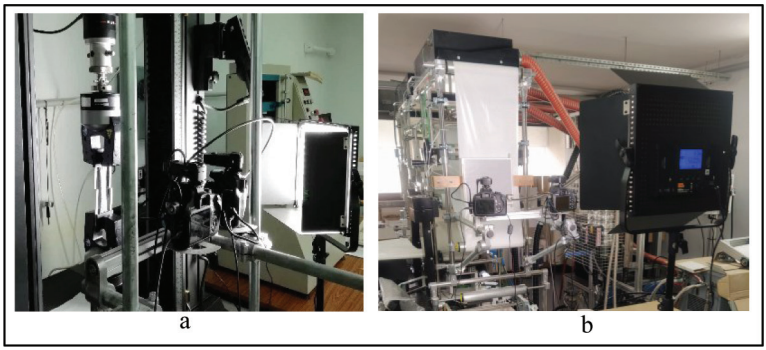

Figure 5. DIC measurement system (a) for tensile test – (b) on the coating pilot.

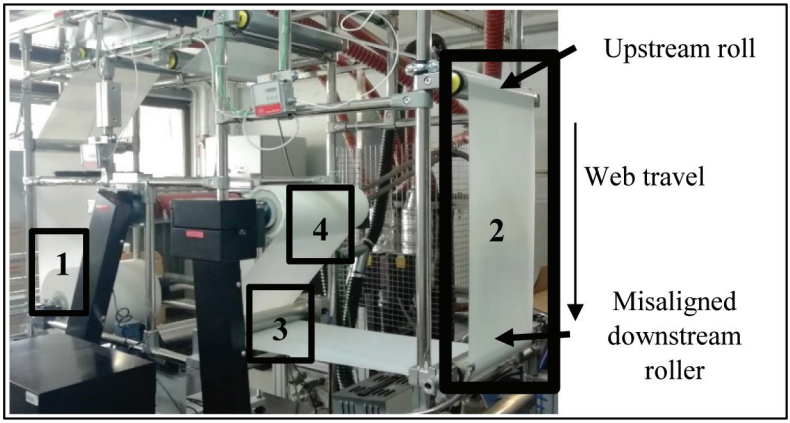

Figure 6. Rotary Coater pilot from RK Coating (1) unwind; (2) studied area with misaligned downstream roll; (3) speed measurement; (4) wind.

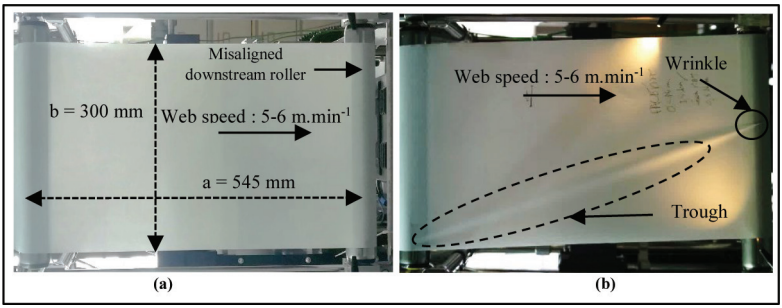

Figure 7. (a) Geometry of the studied area; (b) From troughs (dashed line) to wrinkles (full line) (paper width: 300 mm).

Thus, the appearance of troughs or wrinkles was studied for every couple misalignment angle/web tension. From a geometrical point of view, the paper width is 300 mm for a web span of 545 mm. The web speed was 5.5 ± 0.5 m.min^{-1}, with a web tension between 11 N.m^{-1} and 260 N.m^{-1}. The tram error varied from 0 to 3°.

4 RESULTS AND DISCUSSIONS

4.1 Paper Characteristics

Table 1 below summarises the properties of the papers used, speckled or not. The difference in grammage and thickness between the two reference papers is clear.

Table 1. Characteristics of the tested papers at 23.5 ± 1 °C and 45 ± 5 % HR

Name	*Grammage* ($g.m^{-2}$)	*Thickness* (μm)	*Young's modulus MD* (GPa)	*Young's modulus CD* (GPa)
35 $g.m^{-2}$	36.2 ± 0.2	33 ± 1	8.92 ± 0.88	4.15 ± 1.17
40 $g.m^{-2}$	40.6 ± 0.2	35 ± 1	9.20 ± 0.17	3.93 ± 0.35
35 $g.m^{-2}$ speckled	38.2 ± 0.4	37 ± 1	8.46 ± 0.34	4.27 ± 0.23
40 g.m speckled	42.4 ± 0.2	37 ± 1	9.88 ± 0.33	4.08 ± 0.36

Table 2. Bending stiffness in main directions of tested papers 23.5 ± 1 °C and 45 ± 5 % HR

Name	*Bending stiffness MD* (mN.m)	*Bending stiffness CD* (mN.m)
35 $g.m^{-2}$	0.030 ± 0.014	0.014 ± 0.002
40 $g.m^{-2}$	0.034 ± 0.013	0.016 ± 0.002
35 $g.m^{-2}$ speckled	0.032 ± 0.013	0.015 ± 0.002
40 $g.m^{-2}$ speckled	0.035 ± 0.014	0.017 ± 0.002

It is also important to note that the printing of speckles on the papers has an impact on their weight and thickness. However, regarding the thickness of the speckled papers, it should be noted that despite the different initial thickness, the two speckled papers 35 and 40 $g.m^{-2}$ have the same final thickness (37 ± 1 μm). As for the mechanical properties, the two references, 35 and 40 $g.m^{-2}$, have equivalent Young's MD and CD moduli.

When it comes to the impact of the speckle, it seems that the speckle increases the MD Young's modulus for 40 $g.m^{-2}$ reference and has no statistically significant impact on the 35 $g.m^{-2}$ reference. Table 2 gives access to the bending stiffness of the papers in both directions.

Although there is a difference between the bending stiffness SMD = S_{MD} and SCD = S_{CD} for each reference or speckled paper, it is not possible to make a statistically significant difference between the papers themselves.

The values of the shear modulus $G_{xz,\ Baum}$ are between 2.32 and 2.45 GPa (Table 3). As for the values of the Poisson's ratio $\nu_{xz,\ Baum}$, the values are between 0.18 and 0.20. $G_{xz,\ Baum}$ and $\nu_{xz,\ Baum}$ can be compared with the results obtained with the method derived from the constitutive equations of mechanics for orthotropic materials.

The values of the mechanical constants for water-saturated paper are also measured and determined (Table 4). The Young's moduli are much lower than the values for papers at room temperature and humidity. Variations in Poisson's ratios are also observed.

Table 3. Poisson's coefficient ν and shear modulus G of tested papers calculated following Baum's method

Name	$G_{xz,Baum}$ (MPa)	$\nu_{xz,Baum}$	$\nu_{zx,Baum}$
35 g.m^{-2}	2.35	0.19	0.42
40 g.m^{-2}	2.32	0.19	0.44
35 g.m^{-2} speckled	2.32	0.20	0.41
40 g.m^{-2} speckled	2.45	0.18	0.45

Table 4. Characteristics of the water saturated tested papers

Name	*Young's modulus MD* (GPa)	*Young's modulus CD* (GPa)	$\nu_{xz,Baum}$	$\nu_{zx,Baum}$
35 g.m^{-2}	1.04 ± 0.14	0.15 ± 0.04	0.11	0.77
40 g.m^{-2}	1.13 ± 0.20	0.16 ± 0.05	0.11	0.77

➢ *Determination of Poisson's ratio and shear modulus using constitutive equations of mechanics*

To determine the Poisson's ratio ν_{xz} and the shear modulus G_{xz}, the tangent elastic modulus E_{tan} is plotted as a function of the angle ϕ (Figure 8). Thus, when ϕ = 0°, the samples are tested along MD and when ϕ is equal to 90°, the samples are tested in the CD. Once the curve plotted, the least squares method is applied to compare experimental and model values. In order to highlight the correspondence of the values, parity diagrams are plotted (Figure 9 and Figure 10).

If the match is perfect, a straight line of equation y = x should be drawn. In this case, we have y = 0.99x for the 40 g.m^{-2} paper (R^2 = 0.98) and y = 0.96x for the 35 g.m^{-2} paper (R^2 = 0.99). Therefore, there is a good match between theoretical and experimental values.

The results obtained by this method can be found in Table 5. Note that the values predicted by the Baum model for the Poisson's ratio match the experimental values perfectly. However, this is not the case for the shear moduli where absolute relative errors of 26.79% and 16.24% are calculated.

This underestimation of the shear modulus is also found in the literature, notably in Biancolini's work [29] where significant errors are noted between the experimentally measured values and the empirical values derived from Baum's model. However, in the case of Biancolini's work, it is possible the Poisson's ratios values that have the largest errors.

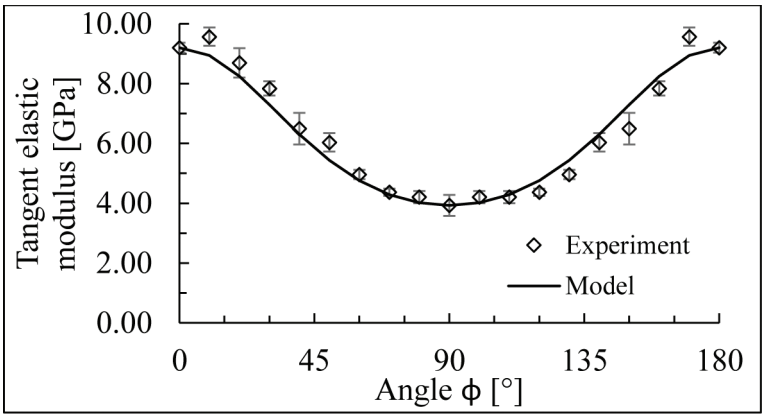

Figure 8. Evolution of tangent elastic modulus versus angle φ for the 40 g.m^{-2} φ is the angle between the tensile test direction and the fiber direction in the paper.

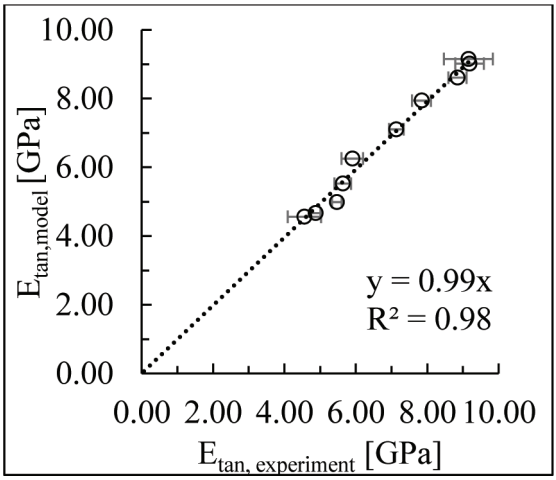

Figure 9. Parity plot of the 35 g.m^{-2}, comparing experimental and modelled data of tangent elastic modulus.

4.2 Wrinkles Observation

Once the wrinkles and troughs have been generated, various points need to be highlighted. First of all, one to many troughs (Figure 11 (a)) are formed at the downstream roll with lengths of approximately 30 to 40 mm. The lengths of the troughs vary until they become wrinkles. As a matter of fact, the troughs gradually

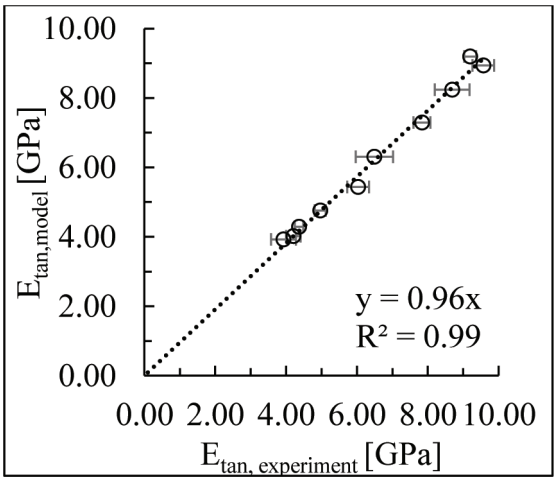

Figure 10. Parity plot of the 40 g.m^{-2} paper, comparing experimental and modelled data of tangent elastic modulus.

Table 5. Poisson's coefficient ν and shear modulus G of tested papers calculated following mechanical constitutive equation and error compare to Baum's method

Name	$G_{xz,exp\text{-}mec}$ (MPa)	*Relative error on* G_{xz} *compare to Baum's model*	$\nu_{xz,exp\text{-}mec}$	*Relative error on* ν_{xz} *compare to Baum's model*
35 g.m^{-2}	3.21	–26.79%	0.19	0%
40 g.m^{-2}	2.77	–16.24%	0.19	0%

grow and reach lengths of approximately 150 mm under certain conditions in favour of wrinkles formations. Finally, when the mechanical limit between no-wrinkle/wrinkle is reached, the troughs have a length between 580 and 590 mm (diagonal on the web span). The next step is the formation of wrinkle. Concerning the appearance of the wrinkles (Figure 11 (b)), they are never parallel to the machine direction of the paper but tilted with an angle α. Before the non-reversible wrinkle formation a trough from the upstream roll to the downstream roll is coming out. This trough starts at the upstream roll, widens to half of the web span before tapering and converging to the downstream roll. As soon as the trough passes the downstream roll, and is still there, it becomes a wrinkle and irreversibly marks the paper.

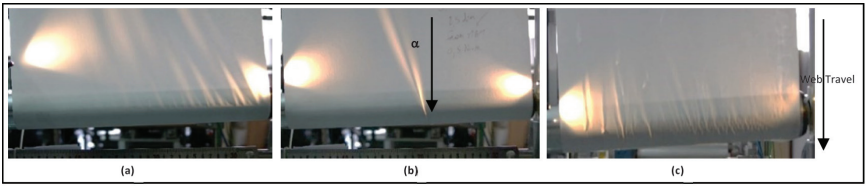

Figure 11. (a) Troughs on uncoated face observed, misalignment angle: 2.5° – Web tension: 150 $N.m^{-1}$; (b) Wrinkles on uncoated face, misalignment angle: 2.5° – Web tension: 260 $N.m^{-1}$; (c) Wrinkles on wet coated face, misalignment angle: 2.5° – Web tension: 80 $N.m^{-1}$.

The last point to look at is the formation of wrinkles on wet paper (Figure 11 (c)). Preliminary tests were performed by wetting the paper just before the web span on which the study is focused. It was found that for a web tension and misalignment angle for which no wrinkles were observed on dry paper (despite the presence of troughs), it was not necessarily the case for wet paper. Wrinkles starts to appear much more easily due to the presence of water.

4.3 Comparison between Experiment and Model

➢ *Experimental data versus modelled data*

Experimental data are presented in Figure 12. They were obtained by looking at the behaviour of the paper web on the coating pilot. A web tension/misalignment angle pair was set, and the paper had a given shape for each pair: flat, slack edge or wrinkled. Thus, the dotted curve with crosses represents the web tension/misalignment angle pairs for which the web remained flat. The dotted curves with triangles and diamonds represent the couples web tension/misalignment angle for which the web had a slack edge and let appear trough. Finally, the dotted curve with squares corresponds to the web tension/misalignment angle pairs for which the web formed wrinkle. Between these curves, hatched areas appear: they correspond to areas where the paper, experimentally, has a certain behaviour (flat, slack edges, wrinkles). Between the curves, some areas remained white and not hatched: these are areas of uncertainty where the behaviour of the paper is not perfectly defined. To summary, the curves define the boundaries between 3 regions related to the wrinkling behaviour of the paper on the coating pilot. These 3 regions are also found in the literature. Region I is for a flat and unwrinkled web which occurs when misalignment is sufficiently small. Region II is for a web with a "slack edge" but no wrinkling which occurs when tension is sufficiently small. However, an out of plane displacement appear. Region III is where the "shear wrinkles" crosses the downstream roll [33].

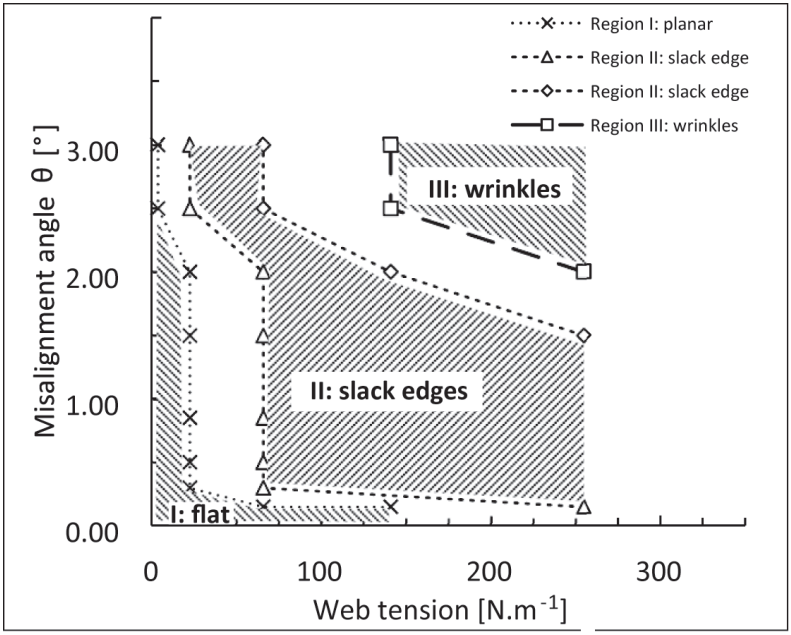

Figure 12. Experimental highlighting the appearance of wrinkles as a function of the pair: web tension – angle of misalignment (35 g.m^{-2} paper, uncoated side).

Furthermore, the results between the coated and uncoated side of the paper were compared to study the influence of the friction coefficient. It has been seeing that differences exist between the areas of regions I and II of each face, especially when the angle of misalignment is greater than 1.5°. Region III didn't appear because no wrinkles could be formed on the uncoated face. This could be explained by the difference in the friction coefficient of the 2 faces of the paper.

The experimental data were compared with the theoretical model for orthotropic materials proposed by [15] (equation 15 and 16). The Figure 13 compares them. In this case, the friction coefficient between paper and roll is unknown. It is a delicate parameter to determine. Thus, this factor was considered as a variable to match as well as possible with the experimental values and to be able to determine the critical tension T_{cr} from which wrinkles can appear (equation 16). It was set at $\mu = 0.2$ as it seems consistent with the observed phenomena.

Concerning the model curve linking the misalignment angle and the web tension, it allows to define areas of wrinkles absence (below the curve) or of wrinkles presence (above the curve). This curve, which corresponds to equation 15, has orders of magnitude equivalent to those present in the literature [10], [15],

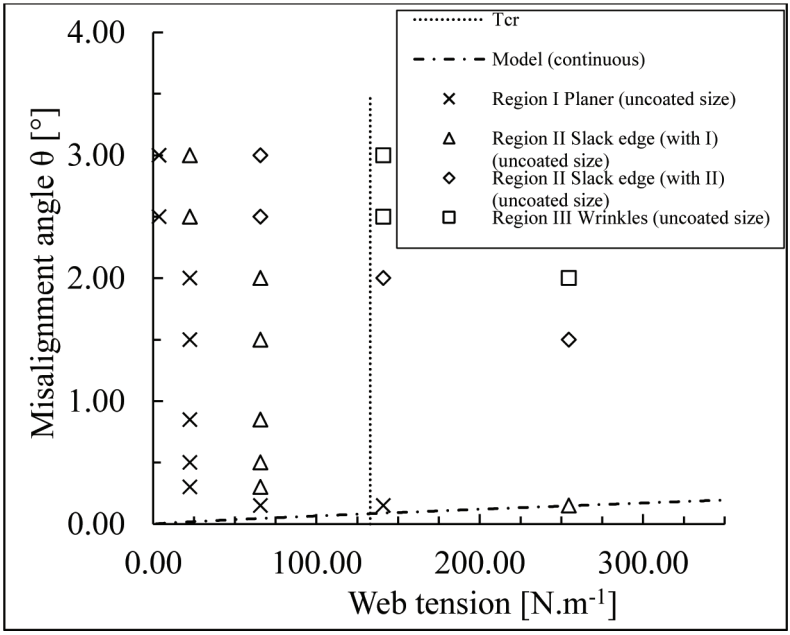

Figure 13. Comparison of experimental and model values for the evolution of misalignment angle versus web tension for dry paper ($\mu = 0.2$) (35 g.m^{-2} paper, uncoated side).

[22] and a similar appearance [34]. However, the experimental values appear to be very high compared to the experimental values generally found [15]. Despite this, the domains defined by the model curves separate the experimental points properly although it includes points where the web has troughs ant not wrinkle. This difference between the experimental and the model might be related to the operator's appreciation of the web wrinkling during the experimental measures.

In addition, a predictive model has also been carried out in the case when paper is coated and considered to be saturated with water. It is well known that mechanical characteristics of wet paper are lower. This prediction was plotted against the prediction of a dry paper (i.e. at ambient humidity, without any external water addition) (Figure 14).

This allowed to define 9 areas, from A to I, in order to help with the coating process. First of all, it should be noted that the critical tension value $T_{cr,water\text{-}saturated\ paper}$ is much lower than the $T_{cr,\ dry\ paper}$ (93% decreasing) This is logical because T_{cr} is directly dependent on Young's moduli which drop drastically when a paper is wet. What is more surprising is that a water saturated paper tolerates misalignment of a roll more easily than a dry paper at equivalent web tension. It is also

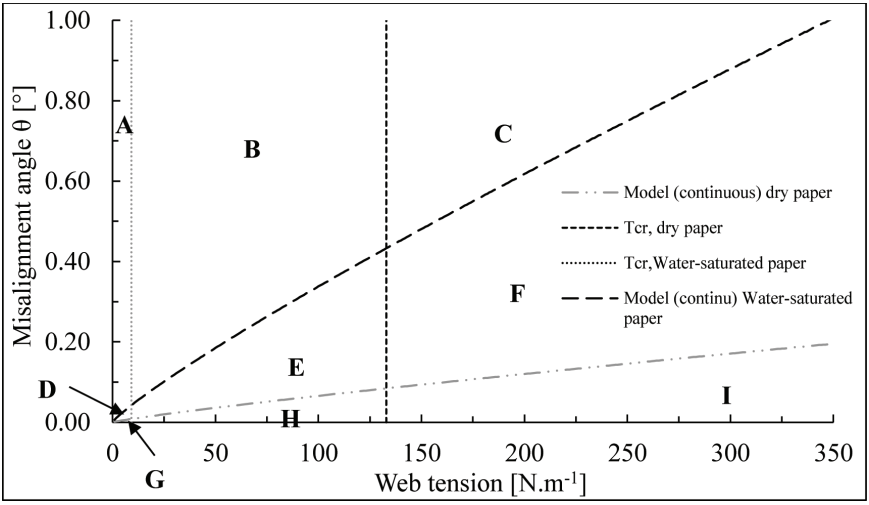

Figure 14. Evolution of misalignment angle versus web tension for dry and water saturated paper (35 g.m^{-2}) ($\mu = 0.2$). Highlighting of 9 areas to facilitate process control.

certain that during a coating process the paper will vary in water content. The case where it is saturated with water corresponds to an extreme limit. Thus, it can be said that the misalignment angle versus web tension curve for a water-saturated paper is a variable boundary depending on the water content of the paper during the process; as well as $T_{cr,water\text{-}saturated\ paper}$. Thus, areas A, D, E, G, H and I are areas where no wrinkles can theoretically occur. Zone B is a wrinkles area for wet paper. Zone C is a wrinkles area regardless of the water content of the paper. Finally, area F corresponds to the appearance of wrinkles for a paper considered dry. This curve model would enable to run a process despite a roll misalignment and without the immediate possibility of correction.

Theoretical considerations have been studied concerning the occurrence of wrinkles in roll-to-roll processes. Through different models and hypotheses, the important parameters to run a process have been, highlighted: web tension, roll misalignment angle and the amount of water in paper. However, the question remains: what are the implications and uses of such theoretical study in an industrial roll-to-roll coating process? The proposed model has already been tested by Gelhbach et al. [13] on an uncoated roll-to-roll system on a laboratory pilot scale. Different materials were used in this study: polyester, polypropylene or crepe paper. The experimental results obtained in this study followed the trends proposed by the mechanical model (equations 15 and 16). In Hashimoto study [15], 2 papers were tested: an uncoated newsprint one and a coated one. For both

papers, the wrinkle/non-wrinkle boundaries modelled by the critical web tension line (equation 16) as well as by the curve linking misalignment angle and web tension (equation 15) correctly isolated the experimental points for which wrinkles appeared. However, unlike Gelhbach, Hashimoto's tests were only carried out on a test bench with few rollers and on an even smaller laboratory scale. Furthermore, these two studies were not carried out in a coating process where rewetting and drying operation are used, unlike the study presented in this article.

Although already experienced, the theory of wrinkling had not yet been tested in a process with unitary coating or drying operations. Thus, the new considerations regarding the role of water may provide insight into how to minimise the risk of wrinkling. Indeed, by installing a complete web control system (measurements, control, actuator (dancer, brake . . .), it is possible to limit the appearance of troughs or wrinkles. In addition, a check of the alignment of the rollers in relation to each other makes it possible to correct their alignment or to conduct the process while being aware of alignment defects. In this second case, the model developed previously becomes very interesting. Knowing the misalignment of two rolls, one with respect to the other, and being unable to correct this problem, it becomes imperative to know the web tension that should not be exceeded in order to avoid wrinkle. It is also important to consider the possible high-water content of the paper, especially after coating. This greatly affects the mechanical properties of the paper and leads to a greater susceptibility to wrinkling. The Table 6 summarises the impact of these parameters and completes the one proposed by Martz [10].

Thus, a production manager is able to produce a figure such as Figure 14 for different areas of the process and know the limits of the different control parameters that should not be exceeded. However, this requires a prior study of the mechanical properties of the paper to be coated and a very precise knowledge of the geometry of the coating machine. This can also have a significant impact on the raw materials consumption by minimising waste and lead to a better process runnability.

Table 6. Impact of water content of paper and misalignment on the appearance of wrinkles (↗: increasing, ↘: decreasing).

Parameters	*Variation*	*Risk of wrinkles*	*Impact*
Water content of paper	↗	*****	↘ Young's modulus and by extension, ↘ critical web tension
Misalignment angle of rollers	↗	***	↘ Critical web tension limit

➢ *Impact of the discretization of the wrinkles number i*

During this study, it was found that making the variable representing the number of wrinkles *i* continuous raise two questions (cf. equation 9). The first of these issues is to ask what is the physical representation of a non-integer number of wrinkles. The second issue is the impact of the discretization of the variable *i* on the model linking misalignment angle and web tension. In order to answer these questions, two figures have been drawn: one for a paper considered dry (Figure 15), one for a paper saturated with water (Figure 16). They represent the evolution of the misalignment angle as a function of the web tension (equation 15) as well as the evolution of the number of wrinkles *i* versus the web tension. They are plotted twice: once considering *i* continuous, once considering *i* discontinuous.

In the case of dry paper, the maximum number of wrinkles in the considered web tension range is 4 (discrete *i*) and less than 4 (continuous *i*). In the case of water-saturated paper, the maximum value is 6 (discrete *i*) and is slightly lower than 6 in the continuous case. Comparing the model curves linking misalignment angle and web tension, it appears that the angle values are alternately overestimated and underestimated when *i* is continuous.

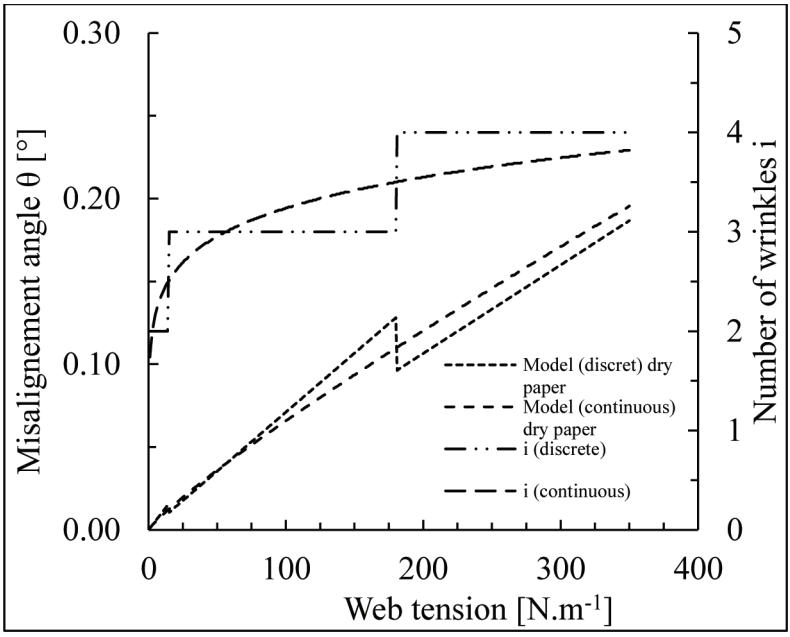

Figure 15. Evolution of misalignment angle and number of wrinkles versus web tension for dry paper (35 g.m^{-2}). Discrete and continuous i.

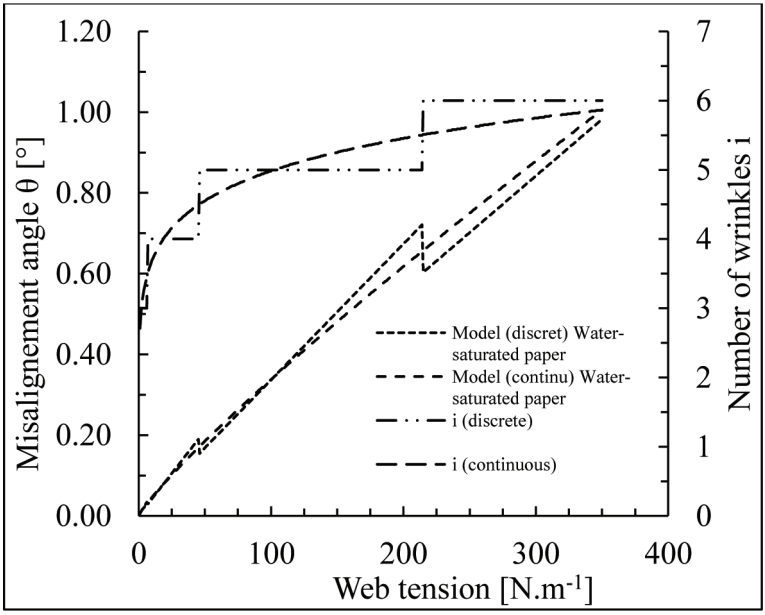

Figure 16. Evolution of misalignment angle and number of wrinkles versus web tension for water saturated paper (35 g.m^{-2}). Discrete and continuous i.

The model curves for discontinuous *i* also show a sharp drop in the permissible angle value. These drops correspond to the appearance of a new wrinkle according to the variation of discontinuous *i*. Thus, these sudden variations can be interpreted as a zone of instability: they are *i* wrinkles and the system tends towards a zone of unstable equilibrium before having *i+1* wrinkle. This would also lead to the following interpretation: having a non-integer number of wrinkles would be a transition phase between two different equilibria. It should also be noted that as the number of wrinkles *i* increases, the range of web tension allowing *i* wrinkles increases.

➢ *Usefulness of the buckling criterion k_c in the case of a process control*

As described previously, the buckling coefficient k_c (equation 16) is used in literature dealing with plates stability under compressive or shear loading. Knowing the aspect ratio β, it is possible to calculate k_c and then to know the critical compression value $\sigma_{z,\mathrm{cr}}$ for which a plate buckles. In the case of buckling due to constrained edges, a similar formulation can be obtained for tensile loading $\sigma_{x,\mathrm{cr}}$. This seems very useful but, what could be the interest of this kind of coefficient in the present case?

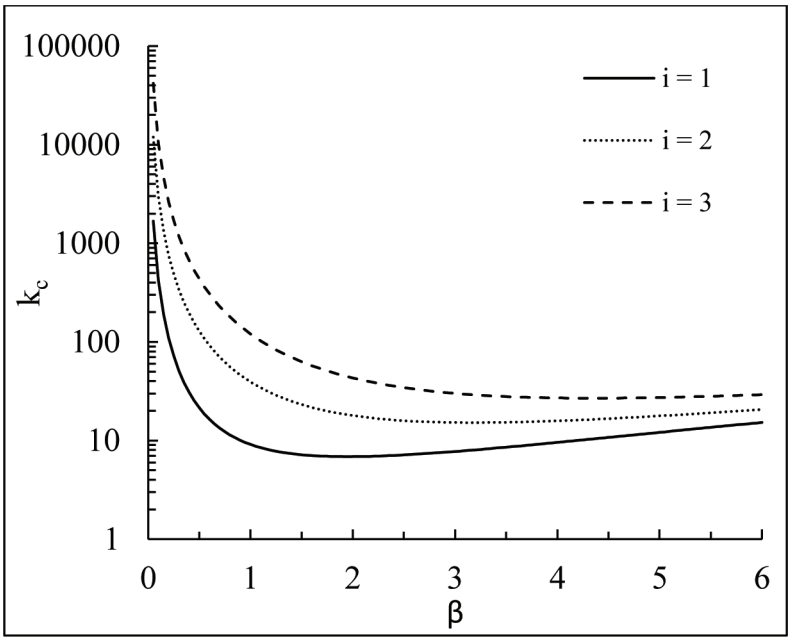

Figure 17. Buckling coefficient k_c versus aspect ratio β.

Based on the work of Zhu et al. [18] and the experimentally determined data, the k_c criterion was determined for different β and *i* (Figure 17). The overall shape of the curves agrees with the literature [18], [25]–[27]. The graph shows that for a large aspect $\beta > 1$ ratio it is easier to buckle the plate than for an aspect ratio $\beta < 1$. Also, for a given aspect ratio, k_c increases with the number of wrinkles on the plate. This means that it will take more stress to form more wrinkles. In this case, the web tension is increasing and then the secondary compressive stress too. However, two points should be kept in mind: in the present study k_c is calculated in the case of a plate in tension where both ends are clamped, and the load is uniformly distributed. However, these two assumptions cannot be applied in the context of the work carried out on the coating pilot (simply supported plate and non-uniform web tension on the width).

Nevertheless, this criterion is in line with the reality of the observed facts. It would just be necessary to review the conditions at the limits and to consider the use of an Airy's stress function for example to determine the evolution of the web tension over the width. Finally, such a criterion would be ideal for an industrial production. It would help to dimension roll-to-roll process by knowing the characteristics of the web. It makes possible to choose the good span between rollers

in order to avoid wrinkles while having a sufficiently large web width to allow the production.

4.4 DIC Analysis

➢ *DIC analysis during a tensile test*

The DIC is used for 2D and 3D image correlation during tensile testing. The aim is to know the displacements and deformations of the sample, especially the out-of-plane displacements. Figure 18 below shows the out-of-plane displacements *dz* of a 35 g.m^{-2} speckled paper sample at 5 different times.

In the rightmost image, corresponding to the end of the tensile test, shortly before breakage, two bands appear. The height of the displacements observed is 200 µm for a width of about 1.5 mm. This corresponds to the out-of-plane deformations of the sample caused by the secondary compressions, induced by the tensile testing of the sample. Zhu et al. [18] found the same phenomenon but much more pronounced on very orthotropic polypropylene films.

➢ *Digital stereo-vision system mounted on the coating pilot for process monitoring*

Adapted system using stereo-vision technology had to be designed in order to enable wrinkles detection and characterisation during processing on the coating

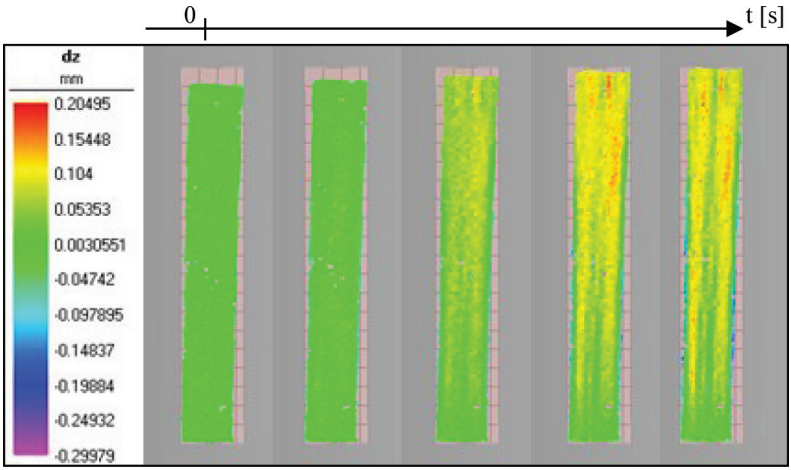

Figure 18. Evolution of the out-of-plane displacement dz (mm) during tensile test CD direction.

pilot. The APS-C (Advanced Photo System type-C) sensors of the two DSLR with the 24 mm focal length of the two lenses give a 49,84 ° horizontal field of view that allows placing the cameras at approximately 35 cm from the characterised paper to visualise the whole width. Considering that configuration and the definition of the DSLR sensors (5184*3456 px^2) the resolution of the digital images is about 63 $\mu m.px^{-1}$. Such a system is compact and might detect and analyse submillimetric wrinkles. The distance and the tilt between the cameras are approximately, and respectively, 30 cm and 30 °.

The stereo-system is mounted on a rigid metallic truss-structure that enables adjustments for clear and sharp images acquisition. DSLR cameras are remotely controlled and energetically autonomous for eliminating every noise after calibration. After installation of the image acquisition system, the first step consists on calibrating the cameras using a chess-board that is located and rotated at different positions and angles every time a picture has been taken. The calibration phase is done once, since the system has not been moved or changed, and give the intrinsic parameters of the DSLRs and the positions and rotations of one camera relative to the other one. Knowing these parameters, it is possible to compute the position of a point in the 3D space if that point is observable on both pictures taken from the two DSLRs thanks to triangulation computation.

A hand-crafted code has been developed in order to reconstruct the surface of the characterized paper thanks to stereo-vision. Difficulties in that project consist on correlating both images since the surfaces to characterised are uniformly diffused whether the wrinkles are not big enough, and computing quickly to correct the pilot behaviour fast enough. At the time of writing, the first difficulty has been resolved by printing or projecting a precise and random speckled pattern on the surface of the paper. Considering the other difficulty, the code is being developed in order to increase the computation speed.

A first experiment of the stereo-system coupling to the computation code is shown in Figure 19. The characterised wrinkle is large, however that test proves the feasibility of the surface reconstruction. The 3D reconstruction (at the centre bottom) was chosen to be fast to compute with a large stereo-grid and small stereo research areas. Because of that last point, it was impossible to find the stereo-correspondent points at the top of the wrinkle (white areas on the figure). Another computation was performed in order to test the resolution of the system: the linear reconstruction of a cross-section of the wrinkle (at the right bottom). The linear profile was chosen to be dense (very thin stereo-grid) with large stereo research areas. The linear reconstruction gave a complete profile of the wrinkle and proves that 3D reconstruction with dense stereo-grids and large research areas might characterise wrinkles that appear on the coating pilot. Tests on smaller sizes of wrinkles are currently performed and multi-threading techniques are currently developed on the stereo-correlation part in order to speed up the process.

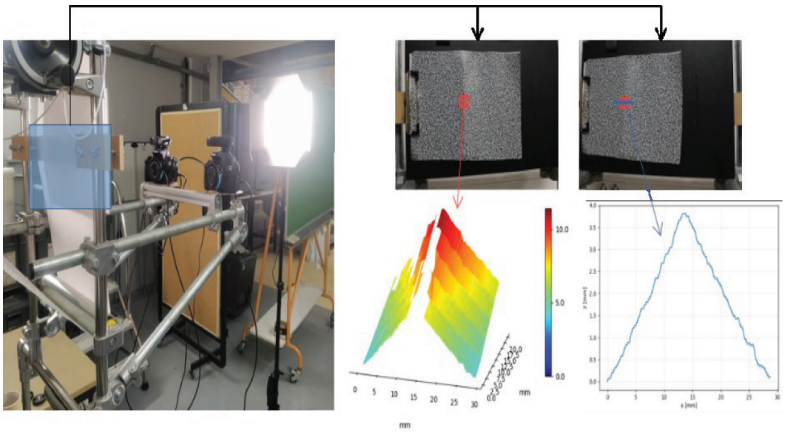

Figure 19. Stereo-system mounted on the coating pilot (left) and printed paper with wrinkle taken from both cameras (top right). 3D Reconstructions (bottom right) have been performed in order to analyse the wrinkle geometry.

5 CONCLUSION AND PERSPECTIVES

In this work, it has been experimentally observed that the appearance of wrinkles during a coating process on a roll to roll pilot depends on different parameters:

- the pair of value web tension – misalignment angle which plays a major role and was already reported in the literature;
- the coefficient of friction between the roll and the side of the paper in contact: that determines the critical tension value at which the wrinkles appear;
- the moisture content of the paper that appears to favour the wrinkles formation.

Moreover, this work permits the comparison of different methods to determine Poisson's ratios and see how these methods can lead to error. It also highlights the impact of discretisation of the variable represented wrinkles numbers *i* on the prediction model. A figure which can help to control a coating process is proposed and also a buckling criterion that may help to dimension the span in a roll-to-roll system. Initial tests of the use of DIC during a tensile test or to monitor the coating process have been carried out. These initial tests are very promising and the development/use of this technique is currently being developed. The perspectives of this work are the improvement of the DIC study on the formation of out-of-plane displacement during a tensile test and during the coating process. Finally, after having determined the friction coefficient between the paper and the roll, a sensitivity study have to be

carry out similar to Martz [10]. By applying these models to an industrial production, it would be possible to avoid the waste of raw material by avoiding folds, and thus improve the runnability of the process.

ACKNOWLEDGEMENTS

Thanks to the IMEP-2 doctoral school for the funding of this PhD thesis. LGP2 is part of the LabEx Tec 21 (Investissements d'Avenir – grant agreement n°ANR-11-LABX-0030) and of PolyNat Carnot Institute (Investissements d'Avenir – grant agreement n° ANR-16-CARN0025-01). This research was made possible thanks to the facilities of the TekLiCell platform funded by the Région Rhône-Alpes (ERDF: European regional development fund). A special thanks to Maxime Terrien and Denis Curtil for their help during this project.

REFERENCES

[1] F. Le Gallic, 'Study of the rheological properties of a starch-based coating color for the production of a multilayer paper insulation', *7th EPNOE International* Congress, Nantes, October 2021.

[2] P. Salminen, 'Studies of Water Transport in Paper during Short Contact Times', PhD Thesis, Abo Akademi, Turki, 1988.

[3] T. J. Walker, 'The taxonomy of wrinkles', in *Tenth International Conference on Web Handling* (*IWEB*), Stillwater, OK, June 2009, p. 15.

[4] J. A. Beisel and J. K. Good, 'The Instability of Webs in Transport', *Journal of Applied Mechanics*, vol. 78, no. 1, p. 011001, Jan. 2011, doi: 10.1115/1.4002116.

[5] W. Tang, J. Chen, and Z. Yin, 'Elastic buckling analysis of webs transported through rollers with misalignment', *Thin-Walled Structures*, vol. 121, pp. 1–7, December 2017, doi: 10.1016/j.tws.2017.09.016.

[6] P. G. Ciarlet, 'A justification of the von Kármán equations', *Archive for Rational Mechanics and Analysis*, vol. 73, no. 4, pp. 349–389, December 1980, doi: 10.1007/BF00247674.

[7] N. Jacques, A. Elias, M. Potier-Ferry, and H. Zahrouni, 'Buckling and wrinkling during strip conveying in processing lines', *Journal of Materials Processing Technology*, vol. 190, no. 1–3, pp. 33–40, Jul. 2007, doi: 10.1016/j.jmatprotec.2007.03.117.

[8] N. G. M. Jacques, 'Modélisation et étude du plissement des tôles lors de leur transport en continu dans les usines sidérurgiques', PhD Thesis, Université Paul Verlaine – Metz, Metz, 2004.

[9] D. Knittel, 'Web dynamics analysis using finite element simulations', p. 6, 2016.

[10] Y. Martz, 'Modélisation et commande de systèmes d'entraînement de bandes flexibles: nouvelles approches à l'aide des éléments finis', PhD Thesis, Université de Strasbourg, Strasbourg, 2017.

[11] Y. Martz and D. Knittel, 'Dynamics of an elastic web in roll-to-roll systems using finite element method', 11th World Congress on Computational Mechanics (WCCM XI) Barcelon, July 2014, p. 12.
[12] J. J. Shelton, 'Simplified model for lateral behavior of short web spans', in *Sixth International Conference on Web Handling* (*IWEB*), Stillwater, OK, June 2001, p. 16.
[13] L. S. Gehlbach, D. M. Kedl, and J. K. Good, 'Predicting shear wrinkles in web spans', *TAPPI Journal*, vol. 72, no. 8, p. 6, Aug. 1989.
[14] J. K. Good, J. A. Beisel, and H. Yurtcu, 'Instability of webs: the prediction of troughs and wrinkles', in *Advances in Pulp and Paper Research*, Oxford, 2009, pp. 517–556.
[15] H. Hashimoto, 'Prediction model of paper-web wrinkling and some numerical calculation examples with experimental verifications', *Microsyst Technol*, vol. 13, no. 8–10, pp. 933– 941, Apr. 2007, doi: 10.1007/s00542-007-0388-z.
[16] J. A. Beisel, 'Single span web buckling due to roller imperfections in web process machinery', PhD Thesis, Oklahoma State University, 2006.
[17] E. Cerda and L. Mahadevan, 'Geometry and Physics of Wrinkling', *Phys. Rev. Lett.*, vol. 90, no. 7, p. 4, February 2003, doi: 10.1103/PhysRevLett.90.074302.
[18] J. Zhu, X. Zhang, and T. Wierzbicki, 'Stretch-induced wrinkling of highly orthotropic thin films', *International Journal of Solids and Structures*, vol. 139–140, pp. 238–249, May 2018, doi: 10.1016/j.ijsolstr.2018.02.005.
[19] C. H. Kim, 'Stress distribution and wrinkling of webs under non-uniform and asymmetric edge loading', *International Journal of Solids and Structures*, vol. 46, no. 3–4, pp. 851– 859, February 2009, doi: 10.1016/j.ijsolstr.2008.09.028.
[20] C. C. Lin and C. D. Mote, 'The Wrinkling of Rectangular Webs Under Nonlinearly Distributed Edge Loading', *Journal of Applied Mechanics*, vol. 63, no. 3, pp. 655–659, Sep. 1996, doi: 10.1115/1.2823346.
[21] C. C. Lin and C. D. Mote, 'The Wrinkling of Thin, Flat, Rectangular Webs', *Journal of Applied Mechanics*, vol. 63, no. 3, pp. 774–779, September 1996, doi: 10.1115/1.2823362.
[22] J. K. Good, D. M. Kedl', J. J. Shelton, and M. Company, 'Shear wrinkling in isolated spans', in *Fourth International Conference on Web Handling* (*IWEB*), Stillwater, OK, June 1997, p. 19.
[23] J. K. Good, J. A. Beisel, and H. Yurtcu, 'Predicting web wrinkles on rollers', in *Tenth International Conference on Web Handling* (*IWEB*), Stillwater, OK, Jun. 2009, p. 36.
[24] S. P. Timoshenko and J. M. Gere, *Theory of Elastic Stability*, 2nd edition. McGraw-Hill Book Company Inc, 1963.
[25] N. Friedl, F. G. Rammerstorfer, and F. D. Fischer, 'Buckling of stretched strips', *Computers & Structures*, vol. 78, no. 1–3, pp. 185–190, November 2000, doi: 10.1016/S00457949(00)00072-9.
[26] E. Puntel, L. Deseri, and E. Fried, 'Wrinkling of a Stretched Thin Sheet', *J Elast*, vol. 105, no. 1–2, pp. 137–170, November 2011, doi: 10.1007/s10659-010-9290-5.
[27] F. G. Rammerstorfer, 'Buckling of elastic structures under tensile loads', *Acta Mech*, vol. 229, no. 2, pp. 881–900, February 2018, doi: 10.1007/s00707-017-2006-1.
[28] C. Fellers and L. A. Carlsson, 'Bending stiffness, with special reference to paperboard', in *Handbook of Physical Testing of Paper*, 2nd edition., vol. 1, 2 vols, New-York: Taylor & Francis Group, 2002, pp. 233–256.

[29] M. E. Biancolini, C. Brutti, E. Mottola, and S. Porziani, 'Numerical evaluation of buckling and post-buckling behaviour of corrugated board containers', Milano, September 2005, p. 14.
[30] G. A. Baum, D. C. Brennan, and C. C. Habeger, 'Orthotropic elastic constants of paper', *TAPPI Journal*, vol. 64, no. 8, p. 5, August 1981.
[31] G. A. Baum and L. R. Bornhoeft, 'Estimating Poisson ratios in paper using ultrasonic technique', *TAPPI Journal*, vol. 62, no. 5, p. 5, May 1979.
[32] J. Viguié, 'Comportements mécanique et hygroexpansif des matériaux ligno-cellulosiques pour l'emballage', PhD Thesis, Université de Grenoble, Grenoble, 2010.
[33] D. R. Roisum, *The Mechanics of Web Handling*, TAPPI Press., 1 vol. Atlanta, 1998.
[34] D. R. Roisum, 'A century of web-handling litterature', in *Eleventh International Conference on Web Handling* (*IWEB*), Stillwater, OK, June 2011, p. 11.

WRINKLES FORMATION AND ORIGINS: FROM THEORY OF WEB HANDLING TO COATING PILOT SCALE EXPERIMENTATION

Florian Le Gallic, Maxime Teil, Jérémie Viguié, Céline Martin and Raphaël Passas

Université Grenoble Alpes, CNRS, Grenoble INP (Institute of Engineering Université Grenoble Alpes), LGP2 (Laboratoire de Génie des Procédés Papetiers) F-38000 Grenoble, France

Torbjorn Wahlstrom Stora Enso

In one of the images at the beginning of the presentation, you mentioned slack edges. Can you also predict slack edge formation with this type of model? If so, could you also explain to me what a slack edge is in the spirit of "mechanics for dummies"?

Florian Le Gallic

First of all . . . so, can we predict slack edge? Yes and no. While doing experimentation, we find out that slack edges appear where we have thought they could, so in a way we can predict it. It is in a previous work that also David Roisum, which is quite known for all his work on the web mechanism, that proposed kind of the same figure that we proposed and it defined a specific area also where we can find slack edges, so in way yes we can find a way to predict slack edges. In answer to your second question, a slack edge is where you have two rollers and a web between and one of the edges of the web is fluttering while the other is under tension. This is slack edges.

Discussion

Torbjorn Wahlstrom

What does the model say about the mechanism behind this fluttering?

Florian Le Gallic

We do not find lot about this and we do not specifically focus on that, so for the moment I could not say more.

Artem Kulachenko Royal Institute of Technology (KTH)

We did the work on slack edges by the way so you can take a look into that, I think it is well described. I have 2 questions. First of all, you use a simple support assumption in your theoretical model, and you say it corresponds to the boundary conditions that you have in your printing system. Why do you think it is the simple support? I mean don't you have free edges anyway?

Florian Le Gallic

Yes, in fact we stay with Good's assumption because it was a bit convenient for us but in fact here we can have free edges too and it means that our system and model still has to be improved but as I say we started with Good's and Hashimoto's assumption to be able to compare our results to and to see how far we are from our the own results, this is the reason why.

Artem Kulachenko

Thank you, and another question, in your very impressive experimental set-up, you have different drying conditions as well. Is it something that you are using, or is it your future work?

Florian Le Gallic

About what condition?

Artem Kulachenko

You have two different driers, you have infrared drying and you have impingement drying, but do you actually use them to see how those affect the wrinkle formation?

Florian Le Gallic

Yes and no. For the experiment I presented today we chose to not dry the paper when we wet it to see the direct impact of water without any drying but we did some coating experiment and in fact it seems that drying has a very important impact which is well known of course: the shrinkage. First of all, we find out after the infrared dryer and just before the hot air dryer that we have one roller that is heating up a lot. It receives a lot of energy so when you touch it you burn yourself. So, we felt that it could lead to a thermal shock and maybe help the formation of the wrinkles and in the channels of the hot air dryer we have also another issues. We have let's say kind of we called orange peels aspect you know on the paper, which is not wrinkled, not the same defect. After coating in the hot air dryer, we are aware that paper is curving and we don't have only wrinkles. So yes, it will be the future step to include the impact of drying.

Niels Vonk Eindhoven University of Technology.

I was wondering, you are projecting the pattern somehow, but this is counter to my understanding of DIC, because DIC is based on tracking grey values in a undeformed and deformed configuration? So how are you keeping the same grey value at the same spot on the X–Y plane? Could you elaborate on this?

Florian Le Gallic

Yes, so about the projections, in fact as I said it is complicated to print a full 2 km rolls in our case because if we do so, it could lead to wrinkles during printing, we want to avoid it and then we need projections. So this DIC part, the specific part under projections and correlations during coating process was a part of project done by my colleague Maxime Teil and using this, as you said, normally we look at the formed and deformed materials but in this case it is a little bit different and we were able to take photos during the coating process, not videos, showing the deformation, so it is a different approach compare to classic DIC but it works and it is the only way for us to monitor the wrinkle formation during the process.

Douglas Coffin Miami University

To induce tension wrinkles, you use a non-uniform tension field and you get that with a misalignment angle but when we are dealing with paper especially wetting it and drying it and putting the coatings on we have a lot of other heterogeneities that can create non-uniform tension, so even with perfect alignment you can get tension wrinkles. How will that change your process operation window?

Discussion

Florian Le Gallic

First of all, we saw this phenomenon because when we try to have most perfectly aligned rollers we still have tension wrinkles. I did not mention it today, but we have tried with 14 gsm cigarette paper and when you wet this – well, I'll let you imagine how it behaves; it is a mess to keep it flat.

So, I think the best solution in this case is to have some more appropriate tension control but for the moment we do not have it because in fact our system is too small to have something industrial. So we are still working on it, we did have contact to see if is it possible to implement other control and measurement of the tension but yes, this is something quite difficult. Maybe another solution could be to control the friction coefficient between rollers and paper because it is also something that, as I show you, has an impact on the critical web tension values, so we can also change it because it could be quite easy to coat and to change the surface of the rollers, so this could be solution.

Douglas Coffin

For the monitoring of the wrinkles online and using the DIC method, there may be other optical methods where you could see the wrinkles and quantify them faster like a Moire fringe pattern or something that might give you faster feedback for control. Have you looked at any other techniques?

Florian Le Gallic

Yes, we also thought about laser profilometry. This will be very convenient, even more so than DIC, but maybe will have less information. So we do not know, we are still investigating this.